



Cite this: *RSC Appl. Polym.*, 2023, **1**, 55

Poly(ionic liquid)s having coumarate counter-anions as corrosion inhibitors in acrylic UV coatings†

Daniela Minudri,^a Anthony Somers, ^b Nerea Casado, ^{a,c} Maria Forsyth^{*a,b,c} and David Mecerreyes ^{*a,c}

Organic inhibitor alternatives to toxic chromium treatments are being sought to protect metal surfaces. One of the limitations of the organic inhibitors is leaching out of the coatings limiting their performance. This work investigates the ionic attachment of coumarate inhibitors into a poly(ionic liquid), polyDADMA coumarate, and its application in a UV-cured acrylic coating. The corrosion protection of the polyDADMA coumarate coating was evaluated by electrochemical techniques including electrochemical impedance spectroscopy (EIS) and surface characterization. The adhesion of the acrylic UV coating formulation onto the steel surface was also investigated. The results showed that the presence of poly(ionic liquid) coumarate in the blend improves the adhesion level as well as providing active corrosion protection.

Received 26th April 2023,
Accepted 29th June 2023

DOI: 10.1039/d3lp00017f
rsc.li/rscapplpolym

Introduction

Corrosion prevention of metals is a relevant practical issue, mainly due to the impact that corrosion damage causes, which results in economic losses and environmental pollution, among others.¹ Mild steel is one of the most useful materials in a diverse range of industries due to its availability and relatively low cost. Furthermore, it can be produced in large volumes and with favorable physical properties such as being ductile and malleable.² These properties make mild steel widely used in marine applications, chemical processing, oil exploration and refining, construction, food industries, and metalworking.³ However, it can also suffer from extensive degradation in these environments, therefore the development of protective methods remains an ongoing challenge for scientists and engineers to avoid the deterioration of mild steel and limit the downstream impacts of corrosion.

Polymer coatings are one of the most proven methods to prevent corrosion, due to their versatility and effective barrier properties. However, most of the current polymer composite coatings are heat-cured organic solvent-based systems which require excessive energy for their fabrication. This process release large amounts of toxic volatile organic compounds (VOCs) during the curing process, causing damaging pollution

to the environment and potential threats to human health. Thus, the development of low VOC releasing, eco-friendly surface coatings with good corrosion prevention performance is a current research focus in the field of metal corrosion protection.⁴ An alternative to the traditional solvent-based thermal processing is the UV-curing technology, which is an environmentally friendly polymerization technique that can be processed without the need for solvents, thereby reducing the hazards resulting from VOC emission, and the process can be done at ambient temperature in a very short time, minimizing the energy consumption.⁵ For these reason, UV coatings are becoming increasingly popular in industrial applications.

One of the most popular methods to protect metal against corrosion is the use of chemical additives that act as corrosion inhibitors (CIs). CIs can diminish the rates of cathodic reduction, anodic oxidation, or both, *via* addition of small quantities of these molecules in aggressive media or coating formulations.⁶ Inorganic compounds such as chromates and dichromate derivates were used as CIs for many years. However, use of these compounds is now prohibited because they are toxic, carcinogenic and harmful to the environment.⁷ Nowadays, organic compounds are being investigated as alternative corrosion inhibitors. Their mechanism of action is based on their adsorption (physical and/or chemical) onto the metal surface to form a protective film.⁸ In this regard, ionic liquids (ILs) are considered an emerging class of corrosion inhibitors which, combined with their good efficiency as CIs, demonstrate several advantages, such as their non-toxic nature, versatility of application and introduction into different coating technologies.⁹

In particular, the use of polymeric versions of ILs (poly(ionic liquids)) as CIs has attracted attention due to the fact

^aPOLYMAT University of the Basque Country UPV/EHU, Joxe Mari Korta Center, Donostia-San Sebastian 20018, Spain

^bInstitute for Frontier Materials, Deakin University, Geelong, Victoria, 3220, Australia

^cIKERBASQUE Basque Foundation for Science, Bilbao, Spain

† Electronic supplementary information (ESI) available. See DOI: <https://doi.org/10.1039/d3lp00017f>



that the polymeric version (*vs.* the individual IL molecule) can provide better adsorption on the surface due to the presence of multiple bonding sites that can interact with mild steel surface.¹⁰ Additionally, the polymeric IL version can displace water molecules from the metallic surface, increasing the efficiency of the CI performance and reducing the likelihood of leaching which is a common problem associated with traditional CIs in coatings. In previous examples, poly(ionic liquids) based on acrylic acid and 1-butyl-3-methylimidazolium acrylate,¹¹ 2-acrylamido-2-methyl propane sulfonic acid¹² and 3-butyl-1-vinylimidazolium bromide¹³ among others, have been investigated as potential CI systems. These poly(ionic liquid)s have demonstrated successful performance for steel protection. Another promising family of CIs are p-coumarate molecules, which demonstrate effective corrosion inhibition due to their good adsorption and interaction with steel surfaces. Recently, the use of different coumarate-based ionic liquids has been reported to show great potential as CI molecules, both in solution and when incorporated in a UV-photo-polymerized coating.¹⁴⁻¹⁷

In the present work, a new poly(ionic liquid) CI, poly(diallyl dimethylammonium) polyDADMA coumarate was investigated including the corrosion protection of steel when incorporated into UV-cured coating formulations. The synthesis of the polyDADMA-coumarate proposed as a corrosion inhibitor offers diverse advantages over previously known coumaric acid-derived inhibitors, such as a simple two-step synthesis that does not contain toxic residues or contaminants for the environment, and can be prepared from commercially available compounds and at relatively low cost. In addition, poly(dimethyl diallyl ammonium chloride) is a well-known strong cationic polyelectrolyte with pH stability and good biocompatibility properties.¹⁸

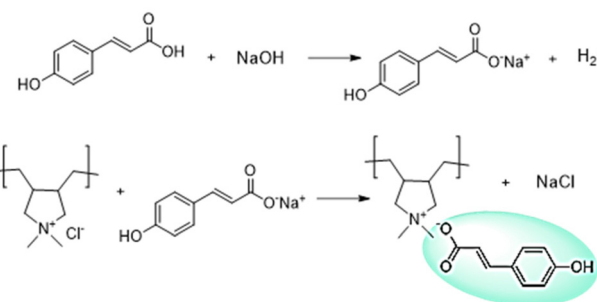
The aim of this research was to investigate the anticorrosive properties of this poly(ionic liquid) and the potential advantages of ionically attaching the coumarate molecule to the polyDADMA polymer chain. The corrosion inhibition performance was evaluated *via* electrochemical measurements, immersion and filiform corrosion tests of coated mild steel AS1020 in 0.01 M NaCl.

Results and discussion

Synthesis and characterization of polyDADMA-COU

Synthesis of the poly(ionic liquid) was carried out *via* anion exchange between commercially available polyDADMA-chloride and sodium coumarate as shown in Scheme 1. As a result of the anion exchange reaction, the polyDADMA coumarate precipitates quantitatively. The chemical structure of the inhibitor was analyzed by FT-IR and ¹H-NMR spectroscopy; the spectra are presented in Fig. 1a and b, respectively.

Fig. 1a shows FTIR spectra of the polyDADMAC (black line) and polyDADMA-COU (red line). The FTIR spectrum of both compounds shows the absorption band 3357 cm⁻¹ assigned to aliphatic secondary amine, and 2940 cm⁻¹ attributed to -CH₂



Scheme 1 Synthesis of polyDADMA-COU.

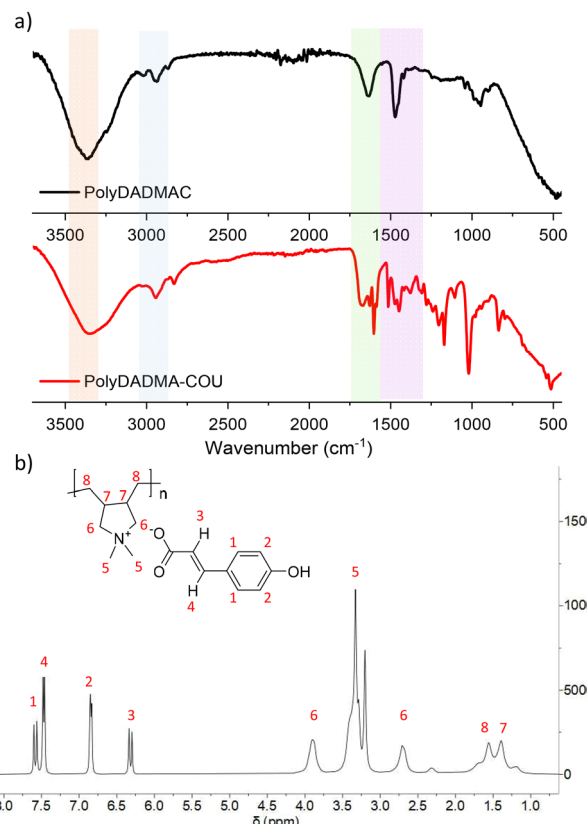


Fig. 1 (a) FTIR spectra of polyDADMA-COU, and (b) ¹H-NMR of polyDADMA-COU in deuterated methanol.

groups, and C-N stretching at 2056, 1283 cm⁻¹ range. Also, the spectra for polyDADMA-COU presented the characteristic bands for the sodium salt carboxylate groups in the vibrational range of 1543–1380 cm⁻¹ (ref. 19) indicating the successful exchange between the Cl anion sodium coumarate. ¹H-NMR spectra of polyDADMA-COU displayed characteristic signals of aromatic carbon atoms at δ 7.55 (d, 2H), 6.89 (d, 2H), 6.36 (d, 1H), 7.48 (d, 1H) and the signals corresponding to poly(diallyl methyl ammonium) at 3.35 (m, 2H), 3.27 and 3.79 (m, 2H), 1.55 (m, 2H), 1.32 (m, 2H), and 1.15 (m, 2H). The integration of the signals confirms the proposed chemical structure and full substitution of chlorine by coumarate anions.



Corrosion protection performance of UV-coatings including polyDADMA-COU

The polyDADMA-COU was formulated into a UV-coating by mixing with dipropylene glycol diacrylate liquid monomer and Speedcure 73 as photoinitiator. By doctor blading a film was formed and monomer mixture was photopolymerized under a UV-light lamp irradiating at a wavelength of 365 nm. The general film formation and UV curing process is illustrated in Fig. 2. The obtained acrylic UV coating was a transparent coating on steel with a thickness of 200 μm .

Electrochemical impedance spectroscopy

Electrochemical measurements were performed to assess the corrosion protection behavior of the coatings; the resulting Bode plots of the coated steel samples with different exposure

duration in 0.01 M NaCl solution are shown in Fig. 3(a) for coating without inhibitor (control), Fig. 3(b, c, and d) for coating containing polyDADMA-COU as CI at 5, 10 and 20 wt% respectively (Fig. S1†). After 24 h immersion, it is evident that both the control coating and the coating containing polyDADMA-COU exhibit good protective behavior, with the values for impedance modulus in the order of $10^6 \Omega \text{ cm}^2$. The impedance modulus determined from the spectra recorded for the control coating and for the coatings containing 5 and 20% of inhibitor decrease with the immersion time, correlating with the degradation process of the coatings. However, coatings fabricated with 10% inhibitor demonstrated opposing behavior, suggesting that the presence of 10% polyDADMA-COU improves the barrier properties of the coating. The stand out performance for polyDADMA-COU 10% may be related to a competition between incorporating enough polymer amount

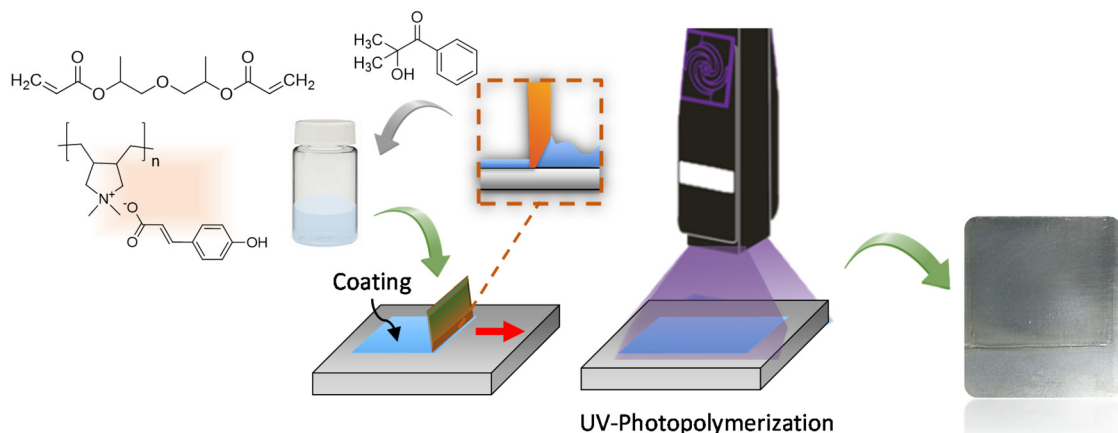


Fig. 2 Coating deposition by Doctor Blade technique of blend containing polyDADMA-COU (5, 10 and 20 wt%), dipropylene glycol diacrylate (80, 90, or 95 wt%), and Speedcure 73 (5 wt%), followed by UV-photopolymerization at a wavelength of 365 nm.

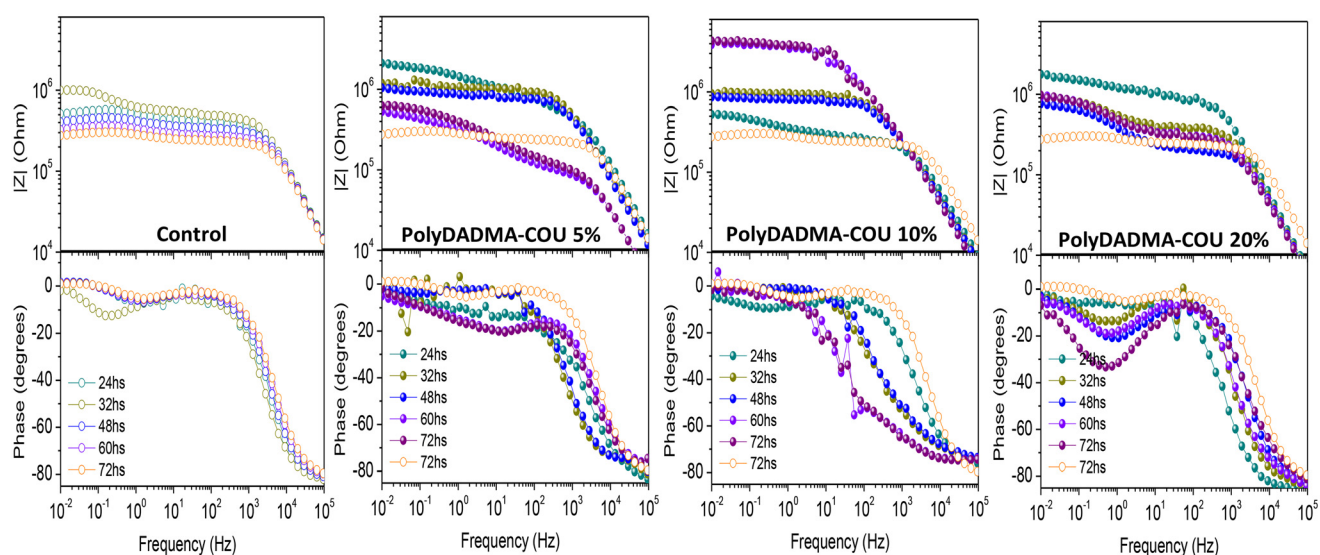


Fig. 3 Electrochemical impedance spectra for different polymer coatings on AS1020 mild steel immersed in 0.01 M NaCl: impedance modulus plots for (a) coating without inhibitor (control), (b) polyDADMA-COU 5 wt%, (c) polyDADMA-COU 10 wt%, and (d) polyDADMA-COU 20 wt%.



to act as CI (differentiating from the control coating) and a small enough quantity to avoid solubility (or inhomogeneity) problems between the inhibitor and the base polymer coating formulation.

The EIS features of coated metal at high frequency are usually related to the barrier properties of the coating, while the low frequency features are typically associated with the metal response during the corrosion process.²⁰ At low frequency the control coating presents an impedance value of $10^{5.9} \Omega \text{ cm}^2$ after 24 h of NaCl solution exposure, with a corresponding phase angle of 13° , and after 72 h the impedance value was $10^{5.4} \Omega \text{ cm}^2$. Mild steel coated with 5% polyDADMA-COU showed an initial impedance value of $10^{6.3} \Omega \text{ cm}^2$, which reduced to $10^{5.8} \Omega \text{ cm}^2$ after 72 hours at the low-frequency range. Similar behavior was exhibited for the coating crosslinked with 20% polyDADMA-COU, where the impedance value for the first 24 hours was $10^{6.2} \Omega \text{ cm}^2$, decreasing to $10^{5.9} \Omega \text{ cm}^2$ after 72 hours, indicating a decrease in protection of the underlying steel.

As well as the resistance, the phase angle (around 80°) of these three coatings (0, 5, and 20% polyDADMA-COU) decreases at high frequencies, which suggests that the electrolyte solution is permeating into the coating and the degradation of the coating is occurring.

In contrast, the impedance modulus at low frequencies for the coating formed from 10% polyDADMA-COU increased from $10^{5.8} \Omega \text{ cm}^2$ to $10^{6.7} \Omega \text{ cm}^2$ after 24 h and 72 h respectively, and the phase angle at high frequencies increased with the immersion time in the corrosive solution. Considering the EIS results, the best performing anticorrosive polymer coating was formed from the blend containing 10 wt% polyDADMA-COU.

In the Nyquist plots of the coated mild steel (Fig. S1†), two semicircles appear after 24 h immersion. The semicircles are not perfect in shape, probably due to the surface roughness, uneven adsorption of the inhibitor, and formation of porous layers on the metal surface. In all cases, the diameter of the semicircle increased with the addition of polyDADMA-COU, indicating that the polymerized ionic liquid can inhibit the corrosion process in the chloride contaminated aqueous solution.

The corrosion inhibition performance of polyDADMA-COU was compared with the behavior of the precursor sodium coumarate (NaCOU) to analyze the effect of the presence of poly(ionic liquid) (PIL) in the blend. When sodium coumarate was incorporated as an inhibitor at 10 wt% (Fig. S2†), the impedance response did not present significant changes with respect to the control coating, and the performance as a corrosion inhibitor is notably less, confirming that the presence of polyDADMA-COU improves the protection properties of the coating.

The equivalent circuit shown in Fig. S3† was used to fit the EIS data using Zview software. The circuit model was used for both control coating and the coating containing polyDADMA-COU, where R_{e} , R_{coat} and R_{ct} are, in order, the electrolyte resistance, pore resistance of the coating, and charge transfer resistance at the interface. It has two capacitive

elements (which were fitted as constant phase elements), one represents double layer capacitance at the interface (C_{dl}) and the other represents the coating capacitance (C_{coat}). The fitting results for the samples after 48 and 72 hours of experiment are shown in Fig. S4 and Table S1.†

From the parameters obtained in Table S1,† it can be seen that the both the coating (R_{pore} and C_{coat}) and metal related properties (*i.e.* R_{ct} and C_{dl}) behave differently in the coating with 10% polyDADMA-COU. Firstly, all coatings containing the inhibitor show higher R_{ct} relative to the control sample, with the highest value being obtained when 10% CI is incorporated into the coating after 72 h of immersion; this indicates the active corrosion inhibition of the polyDADMA-COU.

Furthermore, the coating resistance (represented here by R_{pore}) is highest for the 10% CI material and does not change over 72 h whereas the other coatings all show a decrease in R_{pore} between 48 and 72 h. The C_{coat} values are also consistently higher in the coatings containing polyDADMA-COU than in the control coating; low values of this parameter indicate that the coating allows the electrolyte to penetrate and affect the substrate.²¹ C_{dl} is also higher in the control coating also suggesting the polyDADMA-COU has an active role in protecting against corrosion of the steel substrate as a higher C_{dl} reflects a rougher surface from corrosion attack.

We note that one must be careful with quantitatively over interpreting the EIS data of coated systems, as this methodology has inherent limitations as discussed by Jamali *et al.*²² The fits here also have a significant error due to the scatter in the low frequency data. Nevertheless, taken with the further measurements described below, we can confidently conclude polyDADMA-COU provides additional protection against corrosion in a UV polymerized coating.

Potentiodynamic polarization

The potentiodynamic polarization measurements were carried out after 72 h immersion of AS1020 coated mild steel in 0.01 M NaCl solution, with and without the inhibitor. The polarization curves are shown in Fig. 4. The corrosion parameters such as corrosion potential (E_{corr}), corrosion current (I_{corr}), anodic Tafel slope (β_a), and cathodic Tafel slope (β_c), were calculated using Tafel extrapolation²³ and are summarized in Table 1. The inhibition efficiency ($\eta\%$) was calculated using the following equation.

$$\eta\% = \frac{I_{\text{corr}}^0 - I_{\text{corr}}}{I_{\text{corr}}^0} \times 100$$

where I_{corr}^0 and I_{corr} are the corrosion current densities for coatings without and with the inhibitor, respectively. The decrease in I_{corr} with increasing polyDADMA-COU concentration indicates the corrosion inhibitive nature of the polymer.

The E_{corr} values were shifted towards more positive values for the coating containing polyDADMA-COU with respect to the E_{corr} value for the control coating, at -0.62 V. The E_{corr} values for the coatings containing the inhibitor are -0.60 V, -0.29 V and -0.43 V for the 5, 10 and 20% polyDADMA-COU



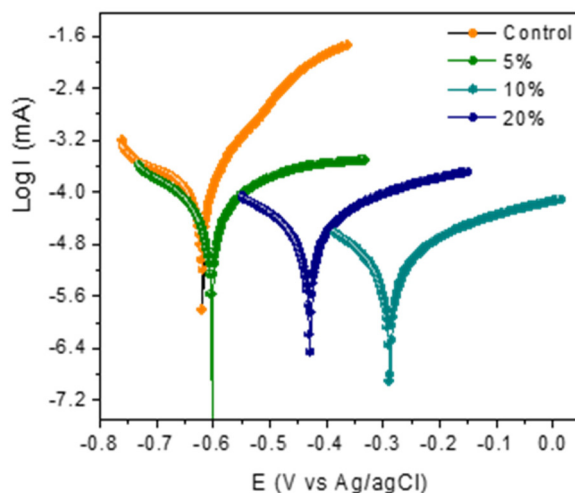


Fig. 4 Potentiodynamic polarization results of AS1020 mild steel after 74 h at OCV in control (orange) and inhibited coatings. polyDADMA-COU 5 wt% (olive), polyDADMA-COU 10 wt% (blue) and polyDADMA-COU 20 wt% (green).

Table 1 Electrochemical parameters derived from potentiodynamic polarization tests on coated AS1020 steel at 25 °C

	$-E_{\text{corr}}$ (V)	β_a (V dec $^{-1}$)	β_c (V dec $^{-1}$)	I_{corr} (mA)	% η
Control	0.62	-14.3	29.0	3.39×10^{-5}	—
5%	0.60	-21.2	19.5	1.32×10^{-5}	61
10%	0.29	-22.3	22.5	1.34×10^{-6}	96
20%	0.43	-22.1	19.5	3.98×10^{-6}	88

coatings respectively, which suggests that the inhibitor is mainly suppressing the anodic reaction (oxidation of Fe to Fe^{+2}), acting as an anodic inhibitor. This is also consistent with the large decrease of current in the anodic arm whereas the cathodic currents all extrapolate to approximately the same values as the control.

The corrosion inhibition efficiencies increased with increasing concentration of the inhibitor from 61% for 5% polyDADMA-COU to 96% for the coating prepared from 10% inhibitor however, for coatings prepared from 20% polyDADMA-COU, the corrosion inhibition was reduced to 88%. It is possible that the dispersion of the inhibitor in the blend at this concentration is less optimal, consequently resulting in more defects and pores in the coating. It is known that the inhibition of the corrosion reaction depends on the better adsorption of the inhibitor molecules on the metal surface. Therefore, it would be coherent to assume that increasing the inhibitor concentration increases the number of adsorbed molecules, which consequently increases the protection of the steel against corrosion. However, the homogeneity of the mixture is also an important parameter. In the case of polyDADMA-COU, the mixing of the inhibitor with dipropylene glycol diacrylate at 20% is not complete and it is possible to observe accumulations of inhibitors in some areas of the coating, resulting in defects and greater permeability of the electrolyte.

The results also show no significant change or trend in cathodic (β_c) and/or anodic (β_a) slopes. This was attributed to the fact that there was no change in the inhibition mechanism by increasing the concentration of the polymer. Coatings formed from blends containing 10% inhibitor showed the best corrosion protection performance, providing an effective barrier with a good ability to compensate for coating defects, and this is consistent with the findings from EIS measurements.

Filiform corrosion test

The protective effect of coatings on mild steel substrates was evaluated against filiform corrosion. For this purpose, the 10% polyDADMA-COU coating was compared with the control coating. This composition was chosen as it displayed the best electrochemical performance as shown above. The scribed specimens were immersed in NaCl solution to activate the corrosion process and, after storage in controlled temperature (40 °C) and humidity, the resulting filiform corrosion was evaluated. Saturated KCl aqueous solution was used to maintain value around 80% of relative humidity inside the container.

Fig. 5 presents the corrosion behavior of coated steel specimens in the presence and absence of the polyDADMA-COU inhibitor. The images indicate that the inhibitor effectively limited filiform initiation and growth. Filiform initiation was evident on the control coatings after one week and a fully rusted surface was observed after one month. In contrast, only some corrosion points were observed on the coating formed with 10% polyDADMA-COU without any evidence of propagation, and these results correlated with the corrosion efficiency discussed above.

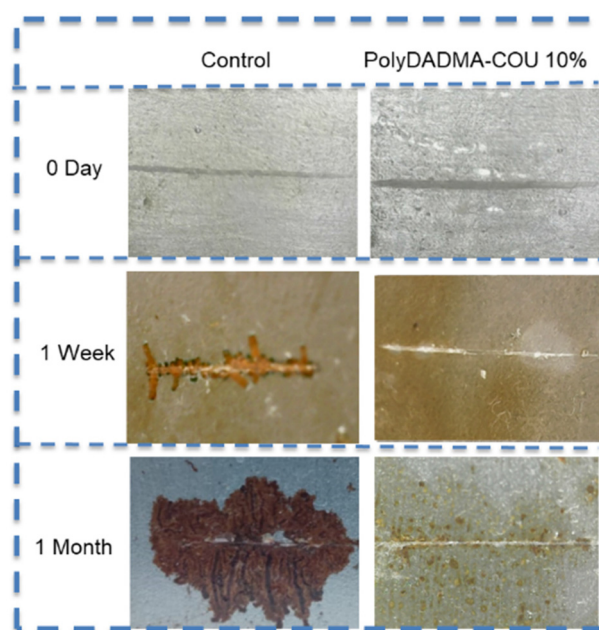


Fig. 5 Filiform corrosion test images of control coating and coating containing 10 wt% of inhibitor.



Leaching test

Leaching test were carried out to evaluate the incorporation and stability of polyDADMA-COU in the polymer coating. Thus polyDADMA-COU containing coatings were compared to reference coatings having 10 wt% of the CI precursor, 10 wt% sodium coumarate (NaCOU), and the control coating without CI addition. The samples were immersed in water for 24 and 48 hours and the water uptake and/or leaching of the ionic coumarate compounds from the UV-cured coatings was studied. As shown in Fig. 6a, the weight of the control coating without ionic additives remained constant after immersion, indicating that neither swelling nor leaching occurred. For the 10 wt% NaCOU coating, a 5% weight loss was observed after 48 hours of immersion, suggesting that leaching of the additive had occurred, which is consistent with the EIS measurements where the corrosion protection performance of the 10% NaCOU coating was similar to the control coating. The 10 wt% polyDADMA-COU coating lost only 2% of its initial weight, providing some evidence of the integration of the inhibitor in the coating.

Adhesion test

Fig. 6b shows the effect of the inhibitor (control *vs.* NaCOU and polyDADMA-COU) on the adhesion of the UV-cured coating, and the influence of polyDADMA-COU concentration was also investigated by comparing coatings formed with 10 and 20% of the CI. Adhesion of the UV cured control coating to the surface of mild steel was the lowest suggesting quite poor adhesion on these metal substrates. Incorporation of both inhibitors increased the adhesion with respect to the control, with the adhesion of the polyDADMA-COU coating being slightly higher than the pre-cursor (comparing the 10% samples), the adhesion was significantly

enhanced for coatings formed from blends containing 20% polyDADMA-COU, suggesting that the presence of polyDADMA-COU improves the adhesion properties of the coating.

Immersion test

Fig. 6c shows the effect of the steel-coated exposition to NaCl solution 24 h, 48 h, and 72 h when a defect is present in the sample. It is possible to see in the optical images obvious corrosion products appeared on the steel surface with the control coating and the rust increased with the immersion time. However, in the case of 10% polyDADMA-COU coating, there are no significant differences in the surface within this time-frame, even with a defect in the coating layer.

Mechanism of corrosion inhibition

The inhibition of the corrosion reaction depends on the adsorption of the inhibitor molecules on the metal surface. In the literature, the linear correlation between the energy level of molecular orbitals and the effectiveness of various organic compounds (such as benzyl imidazole derivatives, amines, and others) as corrosion inhibitors is well known.^{24–26}

From Fig. 7, it can be seen that the E_{HOMO} is located on the heteroatoms and the higher E_{HOMO} value (-11.98 eV) indicate that the molecule has a tendency to donate electrons to appropriate acceptor molecules with low energy empty molecular orbital, which facilitates the adsorption of the inhibitor on the steel surface by affecting the electron transfer processes through the adsorbed layer. The LUMO regions were concentrated on the heteroatoms and benzene rings. The lower E_{LUMO} values (-4.97 eV), the more probable it is that the molecule would accept electrons.²⁷

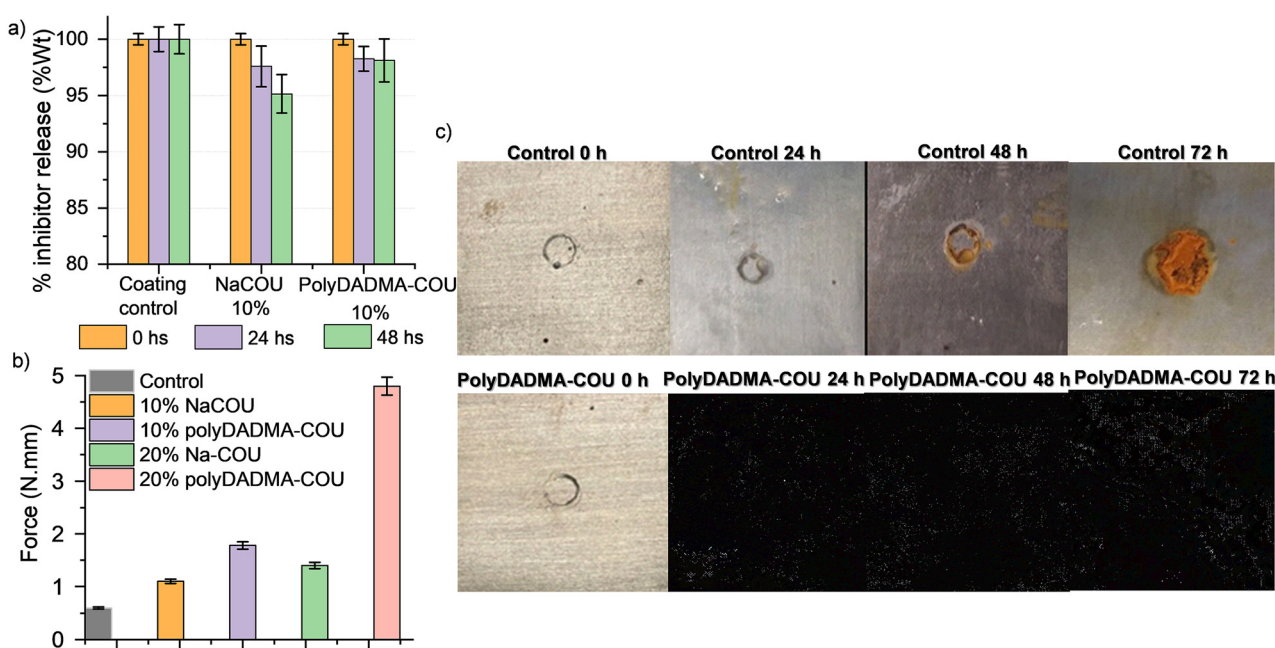


Fig. 6 (a) leaching test of control coating and coating containing inhibitors for 48 h and (b) adhesive force of coated steed with different blends (c) immersion test images for control coating and 10% polyDADMA-COU coating.



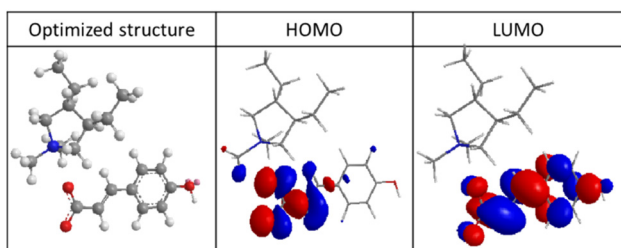


Fig. 7 Optimized structure, highest occupied molecular orbital (HOMO) and lowest unoccupied molecular orbital (LUMO) of polyDADMA-COU.

On the other hand, the value of E_{GAP} provides a measure of the stability of the formed interaction on the metal surface. Low values of the energy band gap (ΔE) lead to good inhibition efficiency because the energy to remove an electron from the last occupied orbital is low, for polyDADMA-COU the $\Delta E_{\text{GAP}} = -7.01$ eV. As explained in the introduction, the macromolecular nature of the poly(ionic liquid) makes that has several binding sites and may have a beneficial effect in the corrosion protection.

Experimental

Materials and methods

Materials. p-Coumaric acid, poly(diallyl dimethylammonium chloride) solution –20 wt% (polyDADMAC) in H_2O , and Darocur (Speedcure 73) were obtained from Sigma-Aldrich. Dipropylene glycol diacrylate was obtained from Arkema/Sartomer. Mild steel AS1020, NaCl aqueous solution, Milli-Q water, methanol, and acetone were used without further purification.

Synthesis of polyDADMA-COU. Synthesis of the poly(ionic liquid) was done *via* an anion exchange reaction between polyDADMAC and sodium coumarate, resulting in polyDADMA-coumarate (polyDADMA-COU). The first step was to convert the p-Coumaric acid to sodium coumarate using a neutralization reaction with NaOH at a 1:1 molar ratio. Then, polyDADMAC was mixed in a necked flask with sodium coumarate in a 1:1 molar ratio, and stirred at 60 °C for 24 h, obtaining polyDADMA-COU. The general synthesis process is illustrated in Scheme 1.

The chemical composition of the synthesized poly (ionic liquid) was analyzed by FTIR and ^1H NMR spectra. ^1H -NMR spectra were recorded on a Bruker AC-400 (^1H -NMR) spectrometer (Bruker, Billerica, MA, USA) and attenuated total reflection – Fourier transform infrared spectroscopy (ATR-FTIR) measurements were performed on Bruker Alpha-P equipment (Bruker, Billerica, MA, USA).

Coating formulation and steel sample preparation. UV-curable coating formulations were prepared using different concentrations of sodium coumarate or polyDADMA-COU (5, 10 and 20 wt%), dipropylene glycol diacrylate (80, 90, or 95 wt%), and Darocur (Speedcure 73) (5 wt%). The inhibitor

was added and mixed in a vial, which was heated at 60 °C overnight to obtain a homogeneous mixture. Mild steel AS1020 surfaces were polished and degreased with acetone at room temperature. The steel surface was coated with the formulation through a doctor blade technique, to produce films with a thickness of 200 μm . The coatings were UV cured over 120 s, using a UVC-5 (DYMAX) UV Curing Conveyor System with an intensity up to 400 mW cm^{-2} , 30 mm lamp-to-belt distance, and belt speed of 7 m min^{-1} . All polymerizations were performed at room temperature and constant humidity.

Electrochemical characterization. The electrochemical impedance spectroscopy (EIS) and potentiodynamic polarization (PP) experiments were conducted using a BioLogic VMP3 multi-channel potentiostat (Biologic, Seyssinet-Pariset, France) combined with EC Lab V10.44 software. In a typical three-electrode cell, the coated mild steel AS1020 (disk of 0.98 mm diameter) was used as the working electrode, a graphite rod as the counter electrode, and Ag/AgCl as the reference electrode; 0.01 M NaCl in water was used as the electrolyte solution.

The PP curves were obtained at a rate of 0.167 mV s^{-1} , with a scan range of –150 mV to 250 mV, relative to the open circuit potential. The impedance response was monitored hourly, over a frequency range from 100 kHz to 10 mHz with 6 points per decade and a sinusoidal amplitude of 10 mV. To ensure the accuracy of the experiment, each test was repeated at least three times.

Filiform corrosion resistance test. A scalpel blade was used to make a 10 mm artificial defect within the polymer coating at the center of each coated surface. The filiform test was adopted from the ASTM standard D2803-03 (ISO 4623). The scribe samples were immersed in 0.1% (w/v) sodium chloride for 10 minutes to activate corrosion. The samples were then removed from the solution and the drops of liquid adhering to it were removed. All the samples were left for a month in a humidity cabinet containing a beaker of saturated KCl solution, maintained at 40 ± 2 °C and $80 \pm 5\%$ relative humidity.

Immersion test. The immersion test was performed in NaCl solutions with the aid of an image processing method to compare the inhibition performance of polyDADMA-COU. A mild steel AS1020 surface of 4 cm^2 was polished and coated with polyDADMA-COU 10% and the reference (dipropylene glycol diacrylate). A circular defect was prepared in the middle of the sample using a punch with a 3 mm diameter. The samples were immersed in a 0.01 M NaCl solution and taken out every 24 h for 3 days. After immersion, the mild steel samples were rinsed with MilliQ water, dried with a stream of N_2 gas, and further dried in a desiccator for 2 h.

Leaching test. Leaching tests were done in three replicates for coatings prepared from 10 wt% sodium coumarate, 10 wt% polyDADMA-COU, and inhibitor-free (control). The samples ($\sim 2 \times 2$ cm) were dried in a dessicator and weighed before being placed in a container with 25 mL of distilled water. The containers were covered to avoid evaporation during the leaching experiments. After 24 and 48 h immersion, the samples were removed from the water and weighed.



Adhesion test. Adhesion measurements were performed using a Texture Analyzer HD plus equipment (Texture Technologies). The adhesion level was related to the peel resistance; the films were photopolymerized on steel and, a PET tape (7 cm × 9 cm) was used to take of the sample as it can be seen in Fig. S5.† For performing the test, the steel was fixed into the lower part of the instrument using tensile grips, and the PET tape was doubled back and clamped to the upper jaw. The adhesion test is the average peel force in N mm obtained during the adhesion test process. The final value was calculated as the average of 4 measurements for each coating.

Computational details

The molecular structure was optimized using the Avogadro and Orca software. Quantum chemical studies were defined based on density functional theory DFT. The calculations were based on 6-31G(d, p) basis set. This basis set provided accurate geometry and electronic properties. After structure optimization, the quantum chemical parameters computed included the lowest unoccupied molecular orbital energy (E_{LUMO}), the highest occupied molecular orbital energy (E_{HOMO}), and energy gap ($\Delta E = E_{LUMO} - E_{HOMO}$) were obtained.

Conclusions

In this work, a new poly (ionic liquid) corrosion inhibitor, polyDADMA polycation having coumarate counter-anions was synthesized and applied as CI additive to an acrylic UV coating formulation. The corrosion protection properties of the UV-cured coatings for mild steel were enhanced with the incorporation of polyDADMA-COU as were the adhesion properties of the coating system on steel. Coatings with 10% polyDADMA-COU as additive showed the highest level of corrosion inhibition, compared to the control and coatings formed from blends containing 5 and 20% polyDADMA-COU. Overall, this novel CI is demonstrated to have a significant potential to protect mild steel substrates when exposed to aggressive chloride ions either in solution or in the atmosphere (as evidenced from the filiform tests). Furthermore, this material could be considered a sustainable solution for improving corrosion resistance of coated steel since uses VOC free UV curing technology and the polyDADMA coumarate CI could be synthesized in water in a simple manner using readily available and inexpensive starting materials.

Conflicts of interest

There are no conflicts to declare.

Acknowledgements

The authors would like to thank the Basque Government for Financial Support through the ELKARTEK 2021 (Project NEOMAT KK-2021/00059). E. U. A. S. and M. F. are grateful for

funding from the Australian Research Council through a Discovery Project DP180101465.

Donation of the acrylic coating Arkema is acknowledged.

References

- B. E. Ibrahimi, J. V. Nardeli and L. Guo, An Overview of Corrosion. Sustainable Corrosion Inhibitors I: Fundamentals, *Methodol. Ind. Appl.*, 2021, **1**, 1–19, DOI: [10.1021/bk-2021-1403.ch001](https://doi.org/10.1021/bk-2021-1403.ch001).
- Y. Peng, A. E. Hughes, G. B. Deacon, P. C. Junk, B. R. W. Hinton, M. Forsyth, J. I. Mardel and A. E. Somers, A study of rare-earth 3-(4-methylbenzoyl)-propanoate compounds as corrosion inhibitors for AS1020 mild steel in NaCl solutions, *Corros. Sci.*, 2018, **145**, 199–211, DOI: [10.1016/j.corsci.2018.09.022](https://doi.org/10.1016/j.corsci.2018.09.022).
- J. Panchal, D. Shah, R. Patel, S. Shah, M. Prajapati and M. Shah, Comprehensive Review and Critical Data Analysis on Corrosion and Emphasizing on Green Eco-friendly Corrosion Inhibitors for Oil and Gas Industries, *J. Bio Tribol Corros.*, 2021, **7**, 107, DOI: [10.1007/s40735-021-00540-5](https://doi.org/10.1007/s40735-021-00540-5).
- M. F. Cunningham, J. D. Campbell, Z. Fu, J. Bohling, J. G. Leroux, W. Mabee and T. Robert, Future green chemistry and sustainability needs in polymeric coatings, *Green Chem.*, 2019, **21**, 4919–4926, DOI: [10.1039/C9GC02462J](https://doi.org/10.1039/C9GC02462J).
- R. Liu, X. Zhang, J. Zhu, X. Liu and Z. Wang, UV-curable coatings from multiarmed cardanol-based acrylate oligomers, *ACS Sustainable Chem. Eng.*, 2015, **3**, 1313–1320, DOI: [10.1021/acssuschemeng.5b00029](https://doi.org/10.1021/acssuschemeng.5b00029).
- E. K. Ardakani, E. Kowsari, A. Ehsani and S. Ramakrishna, Performance of all ionic liquids as the eco-friendly and sustainable compounds in inhibiting corrosion in various media: A comprehensive review, *Microchem. J.*, 2021, **165**, 106049, DOI: [10.1016/j.microc.2021.106049](https://doi.org/10.1016/j.microc.2021.106049).
- Z. Tang, A review of corrosion inhibitors for rust preventative fluids, *Curr. Opin. Solid State Mater. Sci.*, 2019, **23**(4), 100759, DOI: [10.1016/j.cossms.2019.06.003](https://doi.org/10.1016/j.cossms.2019.06.003).
- L. T. Popoola, Organic green corrosion inhibitors (OGCIs): a critical review, *Corr. Rev.*, 2019, **37**(2), 71–102, DOI: [10.1515/correv-2018-0058](https://doi.org/10.1515/correv-2018-0058).
- R. Aslam, M. Mobin and J. Aslam, Ionic Liquids as Corrosion Inhibitors, *Org. Corros. Inhibit.*, 2021, **14**, 315–342, DOI: [10.1002/9781119794516.ch14](https://doi.org/10.1002/9781119794516.ch14).
- M. Taghavikish, N. K. Dutta and N. Roy Choudhury, Emerging Corrosion Inhibitors for Interfacial Coating, *Coatings*, 2017, **7**, 217, DOI: [10.3390/coatings7120217](https://doi.org/10.3390/coatings7120217).
- M. Gobara, A. Saleh and I. Naeem, Synthesis, characterization and application of acrylate-based polyionic liquid for corrosion protection of C1020 steel In hydrochloric acid solution, *Mater. Res. Express*, 2020, **7**, 016517, DOI: [10.1088/2053-1591/ab6000](https://doi.org/10.1088/2053-1591/ab6000).
- A. M. Atta, G. A. El-Mahdy, H. A. Allohedan and M. M. S. Abdullah, Synthesis and Application of Poly Ionic Liquid-Based on 2- Acrylamido-2-methyl Propane Sulfonic



Acid as Corrosion Protective Film of Steel, *Int. J. Electrochem. Sci.*, 2015, **10**, 6106–6119.

13 E. K. Ardakani, E. Kowsari and A. Ehsani, Imidazolium-derived polymeric ionic liquid as a green inhibitor for corrosion inhibition of mild steel in 1.0 M HCl: Experimental and computational study, *Colloids Surf., A*, 2020, **586**, 124195, DOI: [10.1016/j.colsurfa.2019.124195](https://doi.org/10.1016/j.colsurfa.2019.124195).

14 E. Udabe, A. Somers, M. Forsyth and D. Mecerreyes, Design of Polymeric Corrosion Inhibitors Based on Ionic Coumarate Groups, *ACS Appl. Polym. Mater.*, 2021, **3**(4), 1739–1746.

15 E. Aquino-Torres, R. L. Camacho-Mendoza, E. Gutierrez, J. A. Rodriguez, L. Feria, P. Thangarasu and J. Cruz-Borbolla, The influence of iodide in corrosion inhibition by organic compounds on carbon steel: Theoretical and experimental studies, *Appl. Surf. Sci.*, 2020, **514**, 145928, DOI: [10.1016/j.apsusc.2020.145928](https://doi.org/10.1016/j.apsusc.2020.145928).

16 D. Quites, J. R. Leiza, D. Mantione, A. Somers, M. Forsyth and M. Paulis, Incorporation of a Coumarate Based Corrosion Inhibitor in Waterborne Polymeric Binders for Corrosion Protection Applications, *Macromol. Mater. Eng.*, 2022, **307**, 2100772, DOI: [10.1002/mame.202100772](https://doi.org/10.1002/mame.202100772).

17 E. Udabe, M. Forsyth, A. Somers and D. Mecerreyes, Metal-free coumarate based ionic liquids and poly(ionic liquids) as corrosion inhibitors, *Adv. Mater.*, 2020, **1**, 584–589, DOI: [10.1039/D0MA00243G](https://doi.org/10.1039/D0MA00243G).

18 B. Zhang, R. Yao, M. F. Maitz, G. Mao, Z. Hou, H. Yu, R. Luo and Y. Wang, Poly (dimethyl diallyl ammonium chloride) incorporated multilayer coating on biodegradable AZ31 magnesium alloy with enhanced resistance to chloride corrosion and promoted endothelialization, *Chem. Eng. J.*, 2021, **421**, 127724, DOI: [10.1016/j.cej.2020.127724](https://doi.org/10.1016/j.cej.2020.127724).

19 R. Swislocka, M. Kowczyk-Sadowy, M. Kalinowska and W. Lewandowski, Spectroscopic (FT-IR, FT-Raman, ¹H and ¹³C NMR) and theoretical studies of p-coumaric acid and alkali metal p-coumarates, *J. Spectrosc.*, 2012, **27**(1), 35–48, DOI: [10.3233/SPE-2012-0568](https://doi.org/10.3233/SPE-2012-0568).

20 J. M. Sanchez-Amaya, R. M. Osuna, M. Bethencourt and F. J. Botana, Monitoring the degradation of a high solids epoxy coating by means of EIS and EN, *Prog. Org. Coat.*, 2007, **60**(3), 248–254, DOI: [10.1016/j.porgcoat.2007.07.020](https://doi.org/10.1016/j.porgcoat.2007.07.020).

21 X. Liu, J. Xiong, Y. Lv and Y. Zuo, Study on corrosion electrochemical behavior of several different coating systems by EIS, *Prog. Org. Coat.*, 2009, **64**(4), 497–503, DOI: [10.1016/j.porgcoat.2008.08.012](https://doi.org/10.1016/j.porgcoat.2008.08.012).

22 D. J. Mills and S. S. Jamali, The best tests for anti-corrosive paints. And why: A personal viewpoint, *Prog. Org. Coat.*, 2017, **102**, 8–17, DOI: [10.1016/j.porgcoat.2016.04.045](https://doi.org/10.1016/j.porgcoat.2016.04.045).

23 M. A. Amin, K. F. Khaled and S. A. Fadl-Allah, Testing validity of the Tafel extrapolation method for monitoring corrosion of cold rolled steel in HCl solutions – Experimental and theoretical studies, *Corros. Sci.*, 2010, **52**(1), 140–151, DOI: [10.1016/j.corsci.2009.08.055](https://doi.org/10.1016/j.corsci.2009.08.055).

24 K. F. Khaled, Electrochemical investigation and modeling of corrosion inhibition of aluminum in molar nitric acid using some sulphur-containing amines, *Corros. Sci.*, 2010, **52**(9), 2905–2916, DOI: [10.1016/j.corsci.2010.05.001](https://doi.org/10.1016/j.corsci.2010.05.001).

25 J. Fang and J. Li, Quantum chemistry study on the relationship between molecular structure and corrosion inhibition efficiency of amides, *J. Mol. Struct.: THEOCHEM*, 2002, **593**, 179–185, DOI: [10.1016/S0166-1280\(02\)00316-0](https://doi.org/10.1016/S0166-1280(02)00316-0).

26 S. Wang, J. Sun, B. Shan, W. Fan, R. Ding, J. Yang and X. Zhao, Performance of dodecyl dimethyl benzyl ammonium chloride as bactericide and corrosion inhibitor for 7B04 aluminum alloy in an aircraft fuel system, *Arabian J. Chem.*, 2022, **15**, 103926, DOI: [10.1016/j.arabjc.2022.103926](https://doi.org/10.1016/j.arabjc.2022.103926).

27 R. M. Issa, M. K. Awad and F. M. Atlam, Quantum chemical studies on the inhibition of corrosion of copper surface by substituted uracils, *Appl. Surf. Sci.*, 2008, **255**, 2433–2441, DOI: [10.1016/j.apsusc.2008.07.155](https://doi.org/10.1016/j.apsusc.2008.07.155).